Chapter 8

AMORPHOUS SEMICONDUCTORS

Amorphous semiconductors are somewhat of a niche area of electronic materials. However, they are critical to a number of important applications. It would be worth spending some time studying them based on these applications alone. More significantly, these materials are very distinct in their optical and electronic nature. Understanding their properties is highly instructive in a general sense.

Most of the discussion in this chapter focuses on amorphous group IV semiconductors (Si and Ge) which are by far the most commonly applied and technologically important. Amorphous Si (stabilized by hydrogen) is widely used as a photosensitive and photoconductive material in copying machines, for thin film transistors in devices such as flat-panel displays, and for energy conversion in photovoltaic solar cells. Other amorphous semiconductors are primarily chalcogenide glasses. As_2S_3, As_2Se_3, and Te_4Ge are all examples. Some materials occur in both crystalline and amorphous phases, and can be converted from one to the other by proper heat treatment. Such phase transformations have been the basis for data storage devices. Other common amorphous materials include silica (SiO_2) [and related alloys such as common window glass], silicon nitride (Si_3N_4), and most organic compounds. The silicon oxides and nitrides have very large energy gaps and are generally considered insulators, rather than semiconductors. Likewise, organic semiconductors are very different from other amorphous materials and are described in the next chapter.

8.1 STRUCTURE AND BONDING

Amorphous semiconductors can be divided into two general classes, those with tetrahedral bonding and four-fold coordination such as the group IV elemental materials, and those with two-fold coordination as in the chalcogenides (containing group VI elements) and pnictides (containing group V elements).

The structure of the two-fold amorphous semiconductors roughly resembles that of cross-linked organic molecules without the hydrogen. This is not surprising as Se and other group VI atoms are similar to group IV C atoms but with two extra electrons. A carbon chain with two hydrogens per carbon, as in alkane molecules, gets its two extra electrons from the hydrogens, while a Se chain does not need the hydrogens to achieve the same effect. Numerous defects can occur in the chain structures. These are similar to the carbocation and carbanion charged defects in organic chains (see Chapter 9) and have a net charge. The structure of a typical amorphous chalcogenide and some of the common defects are shown schematically in Figure 8.1. The bonding of amorphous chalcogenides is similar to bonding in C chains and results in the same types of molecular orbital structures described in Chapters 4 and 9 for organic molecules. There are also features common to the tetrahedrally bonded amorphous materials described below. We will not consider the chalcogenide materials further as their nature is similar to other more common materials discussed in detail. The interested reader may find additional information in the readings, especially in Brodsky.

The structure of four-fold-coordinated amorphous semiconductors consists of randomly arranged tetrahedra of atoms as shown in Figure 8.2. The bonding is generally covalent, thus this structure is referred to as a random covalent network. Bond distances are close to those of the corresponding crystalline materials (generally $< \pm 1\%$ deviation). The major change is in the bond angle (distortions typically $< \pm 10°$ relative to the tetrahedral 109° 28'). In a diamond-structure crystalline semiconductor, the smallest circuit through individual bonds and back to the starting atom is via six-membered rings. In a random covalent network, the distortion of the bonds leads to anywhere from four to eight membered rings (and occasionally to even more heavily-distorted structures), although the most probable structure is still the six-membered ring. None of the more modest distortions have severe detrimental effects on the optical and electronic properties. The problem comes in the most highly-distorted bonds, and, even more significantly, in dangling bonds resulting from occasional tetrahedra which are left with one corner having no other tetrahedron to bond to. These are rare, but even a few percent of such defects leads to large concentrations of states in the energy gap.

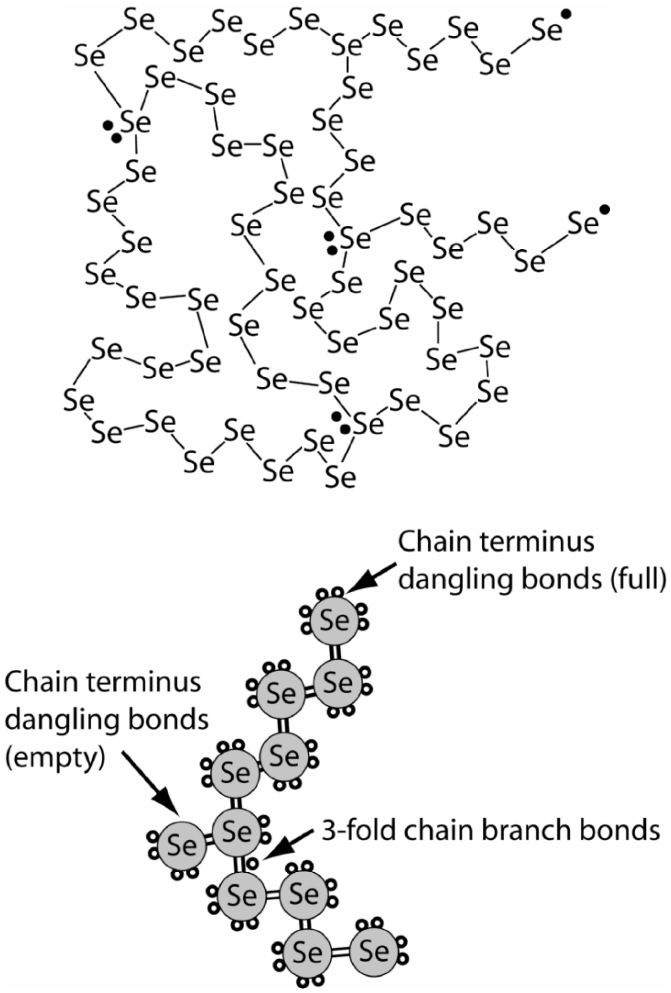

Figure 8.1: Schematic diagrams of the bonding in amorphous Se. Each Se atom is normally linked to two others. Defects occur in which one or three bonds to a Se occur. These junctions have extra electrons or partially-filled states and act as donors as acceptors as a consequence.

If we consider the bonding structure described by the Harrison diagram for Si in Figure 5.4, we find that the weakest bonds are those at the upper edge of the valence band and the lower edge of the conduction band. This is most easily seen by noting that the electrons in the top of the valence-band have the highest energy of those in any filled state. Therefore, one suffers the smallest energy penalty by distorting them.

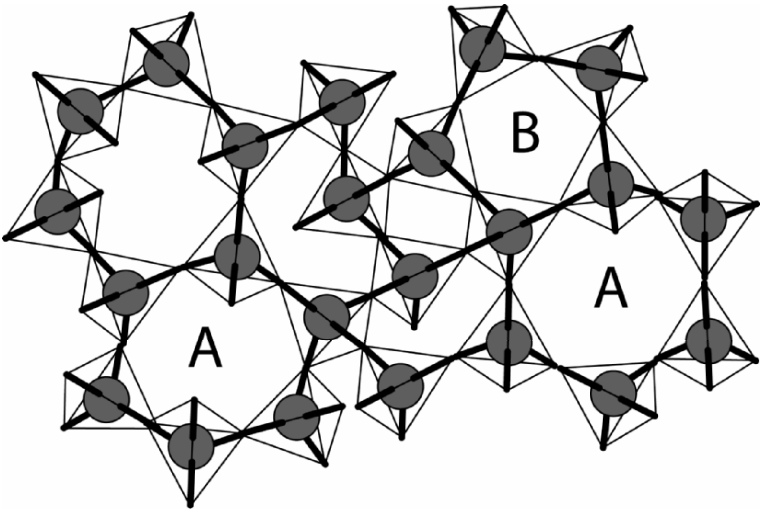

Figure 8.2: Shows a random covalent network of tetrahedrally-bonded atoms such as Si or Ge. Note that the coordination of atoms changes. Some regions show the usual six-membered ring structure found in crystalline materials (rings marked "A") . Other areas contain smaller (for example the five-membered ring, marked "B", or larger rings. It is rare to find rings larger than eight atoms or smaller than four atoms.

A similar argument can be made for conduction band states. Consequently, the bond distortions of the random covalent network are primarily associated with states near the band edge. The distortions further weaken the already weak bonds, raising the energy of the bonding states and lowering the energy of the antibonding states. The higher the distortion, the larger the change in energy and the farther the state moves into the energy gap. The ultimate case of bond distortion is the dangling bond, which results in a non-bonding state near the center of the gap. For the complete random covalent network a continuum of distortions occurs, which gives rise to a continuum of states filling the energy gap. Bonding distortions also modify states throughout the band, resulting in effective local averaging of the density of states. This situation is shown schematically in Figure 8.3.

Several models for the density of states have been proposed and measurements have been made to understand the nature of states in the energy gap of amorphous tetrahedral semiconductors. These generally include the following components: (1) delocalized band-like states, (2) localized band-like states leading to band tails, (3) highly-distorted states deep in the gap, and (4) non-bonding states in the gap. Each of these components is, in some sense, distinct in its behavior, contribution to the density of states, and contribution to conduction behavior, although a sharp boundary may not exist between the groups. Nonetheless, it is useful to make the distinction for reasons we will see below.

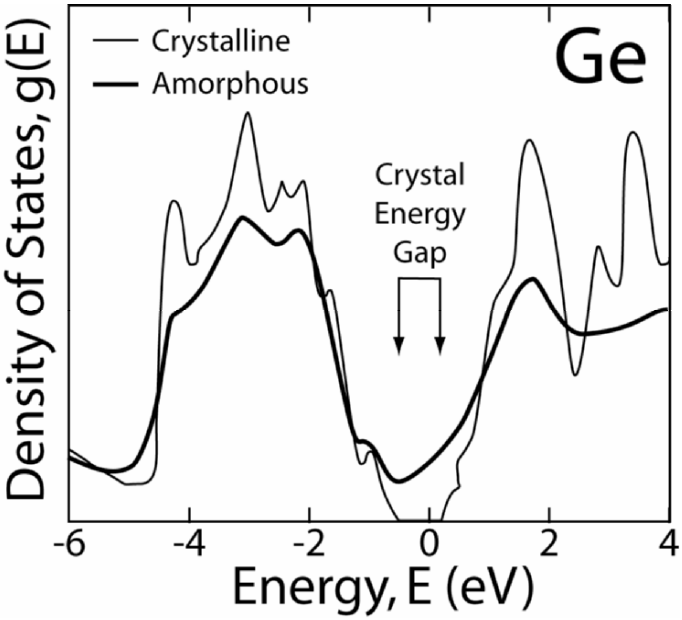

Figure 8.3: The density of states for amorphous and crystalline Ge. Note that the density of states for the amorphous material does not go to zero (there is no true energy gap). Amorphous Si has a similar behavior. Redrawn with permission based on Kramer B and Weaire D., "Theory of electronic states in amorphous semiconductors," Figure 2.8 in Brodsky M.H., *Amorphous Semiconductors* in *Topics in Applied Physics*, v. 36. Berlin: Springer-Verlag, 1979. Copyright Springer, 1979.

Delocalized band-like states are the result of relatively unperturbed bonding-antibonding structures (it does not take much regularity to form them). These account for the bulk of the density of states diagram in the energy range covered by the middle of the crystalline valence and conduction bands. With reference to the LCAO theory of Chapter 5, the relatively undisturbed bond length means the effective matrix elements for any local structure are essentially undisturbed. It is even possible to treat the bulk of the band structure of amorphous semiconductors with a generalized Bloch wave method as in other band structures, although no spherical asymmetry can exist when averaging over the entire material. Electrons and holes in these distributed states move freely at any temperature as they would in a crystalline energy band.

Note that an indirect-gap semiconductor is impossible in an amorphous material as crystalline directions for indirect minima are undefined. Therefore, all amorphous semiconductors have direct gaps.

Localized band-like states are distorted to the point that they lie well away from the energies of the delocalized band-like states. Because localized states are widely scattered in energy and position, they are too far apart to overlap much with each other (true even at third or fourth neighbor distances). Indeed, to be physically isolated from other states of like energy is a *necessary component* of being localized. Therefore, an electron or hole in one such state must change its energy in order to move. If one cooled the material to near 0 K the movement of these carriers would become increasingly sluggish and would finally be due only to long-range tunneling from state to state.

The probability of finding a state of given distortion decreases roughly exponentially with the energy associated with that distortion. Therefore, the density of such states decreases approximately exponentially with energy around the "band edge". This band edge is defined as the transition from localized to delocalized bonding. In principle, this is a nebulous transition. However, because the interaction of states changes exponentially with separation, practically speaking there is a rather abrupt transition between localized and delocalized states. The resulting exponential tails in the density of states within the mobility gap are referred to as Urbach edges. Because the density of states can be expressed roughly as $e^{-(E-E[edge])/U}$, the energy U is characteristic of the width of the tail, and is known as the Urbach energy.

The ability of carriers to move is strongly reduced near the transition from localized to delocalized states, therefore their mobility drops rapidly there. A "mobility gap" can be defined based on this transition for a given amorphous semiconductor. This mobility gap takes the place of the energy gap in crystalline materials. While states exist continuously within the mobility gap, the optical absorption properties and the behavior of diodes based on these materials are governed by the mobility gap in much the same way that the energy gap governs the behavior of crystalline materials. The mobility gap changes with both pressure and temperature, as does the energy gap of a crystalline semiconductor but with a different functional form. The effect is most obvious in the optical gap of the material as discussed in Section 8.4.

The third type of state, deep states in the energy gap are distinct from the band-like localized structures in that their probability ceases to decay rapidly with energy as one draws away from the mobility edge. They represent a "noise background" of states present across the mobility gap at a roughly fixed concentration determined essentially entropically. They are distinct from the fourth type of state as they include a distinct, if very heavily distorted, bond-like character. Such states could include various reconstructions of the interior of a vacancy or multisite vacancy cluster, which would allow dangling bonds to interact at least weakly to form some sort of bond. This situation is shown schematically in Figure 8.4.

Finally, the fourth type of state is the non-bonding dangling bond. Dangling bonds have energies near the middle of the gap where non-bonding states would be

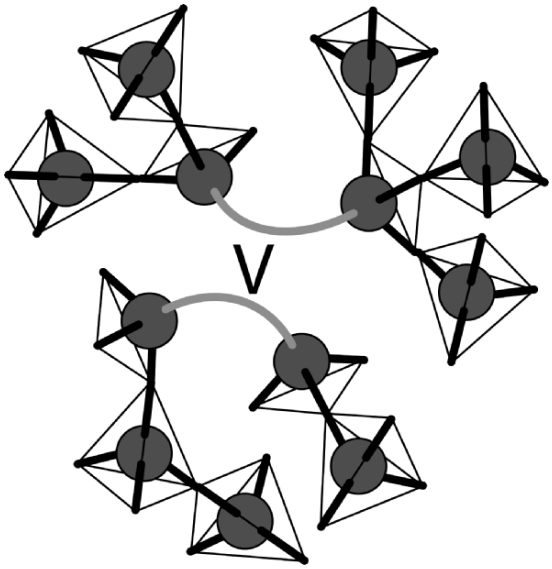

Figure 8.4: Structure of a vacancy in an amorphous semiconductor showing bonding reconstruction.

expected in covalent crystalline materials, as discussed in Chapter 7. Dangling bonds have several important effects on the material. First, they are more common than other deep states in the energy gap as they result from relatively well-defined defects rather than specific rare types of distortions in the structure. Second as non-bonding states they are half filled with electrons. Third, because they are so numerous, they tend to pin the Fermi energy at the center of their energy range. That is to say, it is difficult to move the Fermi energy away from the energy of these defects without either reducing their density or doping the material very heavily. Fourth, because they are non-bonding states, it is possible to insert a small atom (e.g. H) in the structure, which can seek them out and bond to them without otherwise changing the amorphous structure. This is the basis of the stability of hydrogenated amorphous silicon, discussed below.

It is possible to produce some amorphous compound semiconductors such as amorphous GaAs. These materials have a distinction between dangling bonds associated with the cation and the anion. Therefore, non-bonding states of type (4) would not necessarily lie at or near the middle of the mobility gap. In principle, H passivation of such states is also possible. These materials are generally less stable and less homogeneous in amorphous form than other amorphous materials and are not widely used in technology applications.

8.2 HYDROGENATED AMORPHOUS Si

As noted above, adding hydrogen to amorphous Si (or Ge) provides an opportunity for bonding to dangling bonds without affecting the basic amorphous covalent network. Hydrogenated amorphous Si will be designated a-Si:H henceforward. A hydrogen atom, discounting its electron is just a proton and is very small. It can fit into virtually any space in the material including on lone dangling bonds. The hydrogen-matrix bonds have bonding and antibonding levels that lie outside of the mobility gap. This removes most of the effects of dangling bonds, reduces the density of states in the gap overall, (see Figures 8.3 and 8.5) and makes it much easier to move the Fermi level via doping. Hydrogenation also provides significant stabilization of the amorphous structure in Si. The removal of dangling bonds has a direct effect on the density of states not only in the middle of the mobility gap but also at the band edges. Similar results are obtained by adding F. In some cases, optimal results are obtained by adding both H and F together.

One can also consider hydrogen as effectively an alloying element. It has been found, for example, that the mobility gap is directly related to the H_2 pressure in the

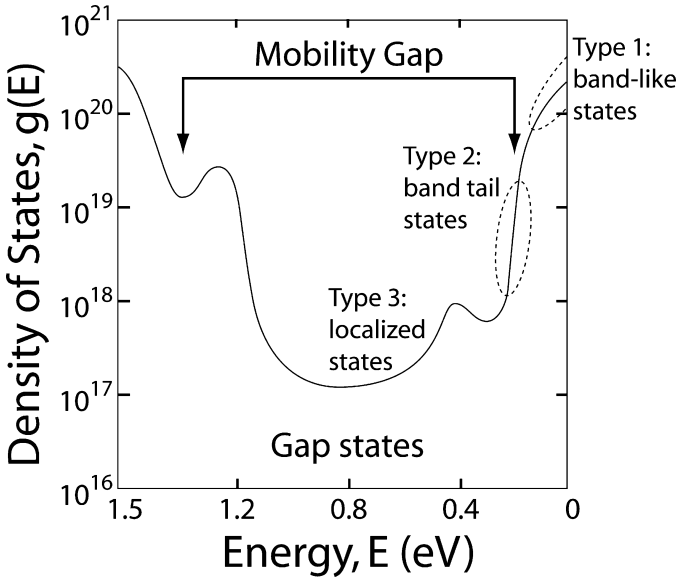

Figure 8.5: Density of states in the mobility gap region of amorphous silicon. Type 4 dangling bond states do not appear in this material because hydrogenation has reduced their density below the highly distorted type 3 localized states. Figure redrawn with permission based on Lecomber, P.G. and Spear, W.E., "Doped Amorphous Semiconductors," Figure 9.1, in Brodsky M.H., *Amorphous Semiconductors* in *Topics in Applied Physics*, v. 36. Berlin: Springer-Verlag, 1979. Copyright Springer, 1979.

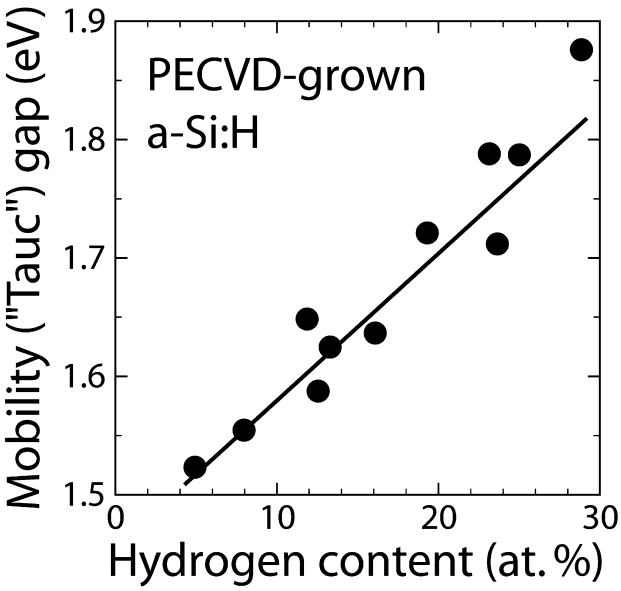

Figure 8.6: The change in mobility gap in a-Si grown by plasma-enhanced chemical vapor deposition as a function of H content. Data courtesy C. Wronski, described in detail in Reference [3].

deposition reactor (Figure 8.6) in a-Si grown by plasma-enhanced chemical vapor deposition. [3] This behavior is also observed in a-(Si,Ge) and a-(Si,C) alloys. Increasing the activity of H_2 in the process increases the probability of hydrogen breaking a highly distorted bond and incorporating into the two broken bonds. This has the net effect of both decreasing the electrical activity of distorted bonds and simultaneously increasing the number of Si-H bonds. Because H is monovalent, its addition fundamentally changes the nature of the a-Si bonding, reducing the need for tetrahedral hybridization and reducing the energy of certain distorted bonding structures. This contributes to increasing the mobility gap.

Unfortunately, Si-H bonds are relatively easily broken (only one single bond needs to be severed) and H is a relatively mobile species. For example, introducing an electron into any Si-H antibonding state eliminates the bond. Once the bond is broken, the H atom may escape into the matrix, leaving an unpassivated dangling bond behind. This results in an increase in electrically active states in the mobility gap under light or forward bias conditions and is known as the Stabler-Wronski effect.[4] In this effect, the density of states in the mobility gap increases upon injection of minority carriers into the material either by photogeneration (as in a solar cell) or by direct injection as in a forward-biased diode. Both of these are detrimental to resulting devices. The effect can be mostly reversed by annealing at moderate

temperatures. This allows repassivation of dangling bonds and a return to better performance. Unfortunately, most devices using a-Si:H involve minority carrier injection and do not operate at sufficiently elevated temperatures to anneal during operation. Thus the Stabler-Wronski effect leads to an overall loss of performance and has been a significant barrier to broader application of a-Si:H. For a detailed description of defect states in the energy gap of a-Si, and a-SiGe alloys, see Cohen in the recommended readings.

Finally, intentional addition of H_2 during a semiconductor growth method such as chemical vapor deposition can increase the density of vacancies and other growth defects because the H_2 can lower their formation energy by reacting with the resulting dangling bonds. This is probably responsible for much of the behavior shown in Figure 8.6. Generally the minimum amount of H_2 necessary to get the job done should be used. On the brighter side, H covers up many growth mistakes that would otherwise degrade device performances even in crystalline materials.

8.3 DEPOSITION METHODS FOR a-Si

Much of the discussion in this chapter refers to changes in the properties of deposited materials as a function of process conditions. Hence, it seems appropriate to mention the relevant methods used in producing a-Si:H briefly. These can be divided into two approaches, chemical vapor deposition (CVD) [see Chapter 12] and sputtering [see Chapter 11], with the CVD contributing the vast majority of the processes. CVD methods, in turn, can be divided into conventional CVD, plasma-enhanced CVD (PECVD) operated either with a dc plasma or an rf plasma, and hot-wire CVD. All of these involve supplying Si (or the atoms for whatever semiconductor is to be deposited) in the form of a gaseous reactant. Typical reactants for a-Si:H are silane (SiH_4), disilane (Si_2H_6) and hydrogen (H_2). In the reactor the reactant, say SiH_4, diluted with H_2, decomposes as in $SiH_4 \rightarrow Si + 2H_2$. The Si then deposits on the substrate as a-Si with incorporation of H atoms depending upon the partial pressure of the H_2 gas in the reactor. This partial pressure also controls the forward reaction kinetics of the source gas decomposition according to the law of mass action [see Chapter 4]. The kinetics and reaction products can be dramatically altered by adding energy to the reactant gases prior to their striking the growth surface. This reduces the need for thermal energy driving the decomposition to be supplied by the substrate surface; which, in turn, reduces the required deposition temperature. Low temperatures are essential to obtaining good amorphous material.

The most straightforward method for supplying energy to the reactants is by passing the gas through a partially- or strongly-ionized plasma. Such plasmas may be generated by dc or rf electric fields. Either may be used in PECVD. When the reactants pass through the plasma, the molecules are ionized, partially decomposed or simply vibrationally excited. Any of these result in a dramatic increase in the reactivity of the molecule. Alternately, hot-wire CVD increases the reactivity of the gas by passing it by a heated filament. This also partially decomposes the reactants.

By choice of reactant, reactant partial pressure, and reaction enhancement conditions, large changes in the details of the reaction process can be achieved. For example, variation of the frequency of excitation of the gas in rf-PECVD changes the types of species present in the gas, which alters the average reactivity. The primary experimental variables in the CVD deposition processes that control aspects such as crystallinity or amorphous nature and defect density in the resulting film are the gas partial pressures, temperature, and the method and conditions of stimulating the reaction.

Sputtering methods use a partially-ionized inert gas such as Ar to bombard a target such as Si. Atoms are knocked off of the target by the collisions and thus vaporized. The resulting Si atoms deposit on a substrate. For low-temperature processes, this results in amorphous material. Hydrogen is supplied by addition of H_2 to the sputtering gas. The sputtering gas pressure determines the number of collisions a molecule undergoes between the target and the substrate. Particles that travel directly from target to substrate without collisions may have significant energies. Collisions generally slow the species, often to thermal energies. This means that the gas pressure influences the growth process dramatically through control of the energy distribution of species striking the growing film surface.

8.4 ELECTRONIC PROPERTIES

8.4.1 Carrier transport and mobility

Free carrier movement in a-Si:H, and to an even greater extent in other amorphous semiconductors, is difficult because there are a large number of defect states in the material into which a free carrier might fall. Once trapped in a defect state, the carrier has several possibilities for further motion, illustrated in Figure 8.7. First, it can gain energy from the heat in the system sufficient to carry it into the delocalized states, in which it is free to move as a carrier in a crystalline material would,

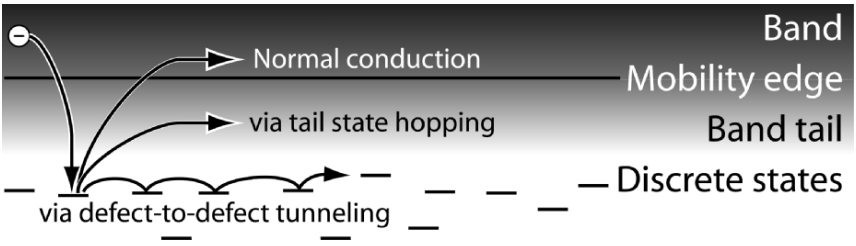

Figure 8.7: Conduction mechanisms illustrated schematically for an electron. Similar processes exist for holes. Normal band mobility requires thermal excitation from a trap state into the band.

although with much higher scattering rate. While it lasts, the mobility of such a carrier is not dramatically different from that of a normal crystalline semiconductor. However, after a short time this carrier is trapped again and becomes effectively immobile. Carriers are excited to the mobility edge mostly from states at or near the Fermi energy. The number of carriers, n for electrons, excited above the mobility edge is therefore given approximately as: [5]

$$n = kTN(E_C)\left(e^{-(E_C - E_f)/kT}\right) \tag{8.1}$$

where E_C is the "conduction band" mobility edge energy, $N(E_c)$ is the effective density of states at the mobility edge, and E_f is the Fermi energy. Mott [6] derived a relationship for mobility corresponding to this carrier behavior and having the functional form:

$$\mu = \frac{C}{T}, \tag{8.2}$$

where C is a constant. Different treatments have derived different forms for the constant but all agree upon the inverse temperature dependence. The models yield typical room temperature mobilities for a-Si:H of the order of 1-10 $cm^2\ V^{-1}s^{-1}$, well above that actually observed. Taken together with Equation 8.1 this model suggests an essentially simple exponential temperature dependence of the conductivity by this mechanism. It also shows that this type of conduction freezes out rapidly as the temperature decreases, especially when, as is typical, the Fermi energy is far from a mobility edge. Band-like conduction is generally only significant at high temperatures or when the material contains a relatively low density of states in the mobility gap.

Conduction can also operate in the band tails below the mobility edge when such tails are wide and have a sufficiently high density of states to allow rapid hopping of a carrier from one site to another via thermally-activated processes. In this case the mobility of a carrier depends exponentially upon the amount of energy it must gain to leave a given state and hop to the next. Thus, it was proposed that the mobility will have the form [5]

$$\mu_{hop} = \frac{q\nu_{ph}R^2}{6kT}e^{-W/kT} \tag{8.3}$$

where ν_{ph} is the average phonon vibrational frequency of the structure, q is the electron charge, R is the hopping distance in an average hop, and W is the energy gain necessary for the average hop. The net mobility is a weighted average over all states and the weighting factor is determined by the effective density of states at a given energy. The density of states typically falls rapidly (exponentially) below the mobility edge, while the probability for the energy gain decreases exponentially as the barrier for the hop becomes larger. The net result is equivalent to what one would obtain directly from Equation 8.3, using W=kT, leaving the exponential term as 1/e. Note that once again, as in Equation 8.2, the mobility decreases roughly inversely

with temperature but with a different constant. The mobility obtained is of the order of 0.01 $cm^2\ V^{-1}s^{-1}$ for typical values of the remaining constants, or about two orders of magnitude smaller than for the conduction above the mobility edge. The band tail mobility is closer to typical values observed for mobilities.

In the final conduction pathway is phonon assisted tunneling. This requires states sufficiently close in energy and momentum and physically close enough in the solid for tunneling from one to the next to occur. The farther the carrier energy is from the mobility edge the slower this process, in general, due to the lower density of states and the higher the effective tunneling barrier. However, in some cases tunneling may be faster than for the mechanisms discussed above. In particular, if there is a relatively high density of states at the Fermi energy then this mechanism can operate relatively easily. Such a situation is typical when the Fermi energy lies at the energy of dangling bond states and when there are many dangling bonds present in the material. As with hopping in band tails, the phonon-assisted tunneling mechanism conduction has a highly path-dependent effective mobility. Carriers that tunnel between states that are very close to one another in the solid move rapidly and have a higher effective mobility. More widely spaced states result in extremely small effective mobilities. The jumping rate, r, is given by [7]

$$r = \nu_{ph} e^{-W/kT} e^{-2\alpha R}, \tag{8.4}$$

where tunneling yields the exponential dependence of rate on jump length R, α is the characteristic decay length of the integrated overlap of the wave functions of the two states, and W represents an effective energy barrier. In this case, W is assumed to be modest. From Equation 8.4 an effective mobility can be estimated as [7]

$$\mu = \frac{qR^2}{6kT} r = \frac{q\nu_{ph}R^2}{6kT} e^{-2\alpha R} \quad e^{-W/kT}, \tag{8.5}$$

which is obtained by noting that the diffusivity is $D=rR^2/6$, and using the Einstein relation, $\mu=qD/kT$. Equation 8.5 is nearly identical to Equation 8.3, with the exception of the addition of the exponential tunneling term and includes the same inverse temperature dependence as in the previous formulae. This would be convenient if it were not for a much more complex behavior in the average jump distance R. Furthermore, the necessity to weight the probability of each jump for the likelihood of occurrence of a given configuration of states of a given type causes a very different net temperature dependence. A complete derivation is beyond the scope of this book but may be found in Mott [7]. A properly averaged jumping rate gives a term of the form:

$$r = \nu_{ph} e^{-A/T^{1/4}}. \tag{8.6}$$

A temperature dependence of the conductivity scaling as an exponential of $T^{-1/4}$ is a standard signature of variable-range phonon-assisted tunneling conduction. A similar behavior is found for conduction in bands of defect states in crystalline semiconductors.

8.4.2 Mobility measurements

A standard method to determine the mobility of carriers in semiconductors is the Hall effect. In this method, a current passes through a sample, which is subjected to a magnetic field normal to the conducting plane. The Lorentz force deflects the moving carriers in the plane, resulting in a voltage build-up perpendicular to the moving current. The sign of this voltage gives the type of carrier moving, while the magnitude gives the mobility. For variable-range hopping, this behavior is very unpredictable, as either electrons or holes may dominate the conduction process. This is because the carriers move through states near the Fermi energy. Consequently, it is nearly as easy for electrons to move as for holes. Whichever carrier has the higher probability of hopping from state to state will dominate. This shifts as temperature changes, leading to instabilities in the measurements.

An alternative method of measuring mobility is to determine how far photogenerated charge in a sample drifts in the presence of an electric field as a function of time. The experimental method for such measurements is shown schematically in Figure 8.8. An electric field is applied along the length of a bar of sample. A flash of illumination creates electrons and holes. These drift in opposite directions according to their mobilities, the applied electric field, and time, resulting in a current at the contacts as carriers arrive. This current may then be modeled to extract the mobility. Because the carriers are charged, a voltage difference is associated with the separated charges. This voltage may also be sensed at contacts along the test material. In a crystalline semiconductor with a well-defined carrier mobility, the carriers drift together down

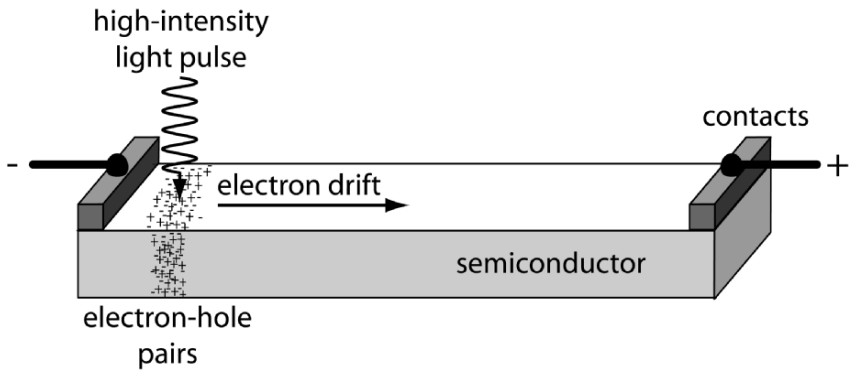

Figure 8.8: A schematic diagram of the method for making drift mobility measurements. Current is measured to determine the number of photogenerated carriers reaching the contacts per unit time.

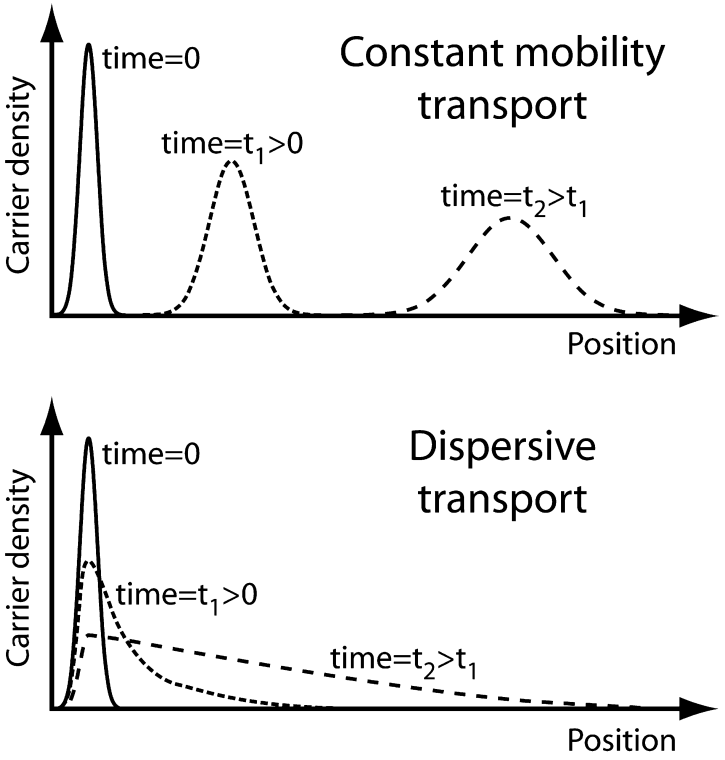

Figure 8.9: Schematic diagram of the typical distribution of carriers in a drift mobility measurement of an a-Si:H sample for several times. [For details see Zallen, Ref. 8.]

the sample in a bunch. The bunch spreads out due to diffusion while recombination eliminates minority carriers gradually. The net result is the carrier density as a function of time shown in the upper part of Figure 8.9 for normal conduction.

In an amorphous semiconductor the carrier mobility varies dramatically from one carrier to another. When these carriers drift in an electric field the result is very different from in a crystalline material and the distribution for this "dispersive transport" is shown in the lower half of Figure 8.9. The most common situation is that a carrier has no significant mobility (most carriers are trapped), thus the peak in the concentration of carriers is fixed at its initial location. A fraction of the carriers become mobile and drift in the field according to the mechanisms outlined in Figure 8.7. Even though the most common location of carriers is where they started, the

average position moves. The behavior is referred to as dispersive transport because there is a dispersion in the mobility values.

Experimental measurements of carrier mobilities in a-$Si_{1-x}Ge_x$:H alloys show that the mobility decreases [9] and the defect density increases [10] exponentially with x. Deposition temperature, post deposition annealing temperature, hydrogen partial pressure during deposition, photon flux, and other variables affect both mobility and defect state densities in complex ways. Most of density of states changes can be traced to the concentration of hydrogen in the material and its interaction with dangling bond states, which are strongly affected by the experimental variables. For a more detailed discussion, see the recommended readings.

8.4.3 Doping

A significant problem in application of amorphous materials including a-Si:H is doping. Doping, as discussed in previous chapters, involves adding impurity atoms that change the total number of electrons (and protons) in the material and shift states near the band edges. These are the same states that are typically affected by distortions of the bonding so one might expect that the behavior of a dopant might be altered by the amorphous nature of the structure. Even more likely to cause problems is the very high density of defects. Each defect can potentially compensate for a dopant atom, as was the case for vacancies in crystalline semiconductors. Considering the intrinsically defective structure of amorphous semiconductors, it is not clear that addition of monovalent substitutional impurities used in doping crystalline materials should in fact lead to electrically-active states. A dopant atom having an extra electron is an ideal candidate for location on a three-fold-coordinated defect site in the amorphous covalent network. Therefore, it would not be surprising if a dopant atom added during the deposition process would simply induce formation of a defect site, as was the case for doping partially ionic semiconductors. In spite of these concerns, a significant fraction of dopant atoms have been observed to be electrically active. This is presumably because either most of the dopants are in tetrahedrally coordinated sites, or adding dopants adds fewer additional coordination defects to the material than the number of dopant atoms. The complexity of the materials makes prediction of doping effectiveness from theory nearly impossible so it is useful to look at the experimental data.

A-Si:H and related materials are typically doped with B, As and P, as is crystalline Si. These dopants have a very high solubility in both the amorphous and crystalline phases and can be electrically active to concentrations exceeding 10^{20} cm^{-3}. Typical defect densities in the mobility gap range from 10^{17} - 10^{19} cm^{-3} eV^{-1} and vary with deposition technique. Therefore, the possibility of doping depends somewhat upon the details of the material processing, making process control critical to the yield of resulting devices. Nonetheless, if the electrically active dopant concentration were 10^{20} cm^{-3}, then one might expect reasonable doping. In plasma-enhanced chemical vapor deposition and similar vapor phase processes, roughly 1/3 of the dopant atoms incorporated into the amorphous structure are electrically active. In PECVD, doping

is generally accomplished by adding gases such as diborane (B_2H_5), arsine (AsH_3) or phosphine (PH_3) to the deposition environment. One can also ion-implant the dopant into a-Si:H, but the efficiency of the doping that results is low, even when the implant is carried out at elevated temperatures. Doping by addition of phosphorous or boron to a-Si:H by MOCVD generally allows changes in conductivity in excess of five orders of magnitude, although the Fermi energy rarely is less than 0.2 eV from the mobility edges. Nonetheless, the built-in voltage in an a-Si junction may exceed 1 V. Even with an optimal process, it is difficult to obtain a sufficiently high electrically active dopant concentration to move the Fermi energy all the way to the mobility gap edges which would yield the full 1.5eV built in voltage one might expect based on the mobility gap value.

A consequence of the difficulty of doping is that most a-Si:H devices are based on "p-i-n" structures. In these, one dopes the ends of the device as strongly as possible, leaving the central region undoped (intrinsic). The highly doped regions are used to generate depletion, built-in electric fields, and for effective contacts to the material. The central intrinsic region is generally the "active" part of the device as in a solar cell or field-effect transistor. The reasons for the p-i-n structure include the fact that optimization of the material for high doping may not lead to the best properties for stable operation of the device. With the p-i-n structure, the intrinsic region can be produced under conditions favoring higher or more stable device performance.

8.4.4 Short-range order

The most straightforward method to obtain high doping levels is to use polycrystalline rather than amorphous material for the heavily doped regions. The difficulty with polycrystalline Si is that, when lightly doped or undoped, the properties and performance are heavily influenced by grain boundaries. The density of such boundaries is determined by the deposition technique and conditions used, which renders lightly-doped or intrinsic polycrystalline materials unpredictable or unreliable for devices. The solution to both the doping problems of a-Si:H and the unreliability of lightly-doped or intrinsic polycrystalline Si is to use polycrystals for heavily doped regions and in conjunction with the contacts, and amorphous material for the lightly-doped or intrinsic areas.

One does not need to obtain large grain sizes in order to produce a much more dopeable material. Thus, the standard contact regions in current a-Si:H devices use a heavily-doped micrograined or nanograined polycrystalline material. Recent experiments by Feng et al. have further demonstrated that such nanograined material can be controllably obtained by simple changes in the deposition conditions for sputter-deposited a-Si:H. [11] The process uses dc magnetron sputtering [see Chapter 11] with a Si target with a mixture of Ar and H_2 gas. Crystallinity increases as hydrogen partial pressure increases above a critical pressure, which depends upon the details of the processing equipment, over a range of temperatures. It is also straightforward to produce amorphous C-Si-Ge alloys this way by mixing CH_4 with the sputtering gas

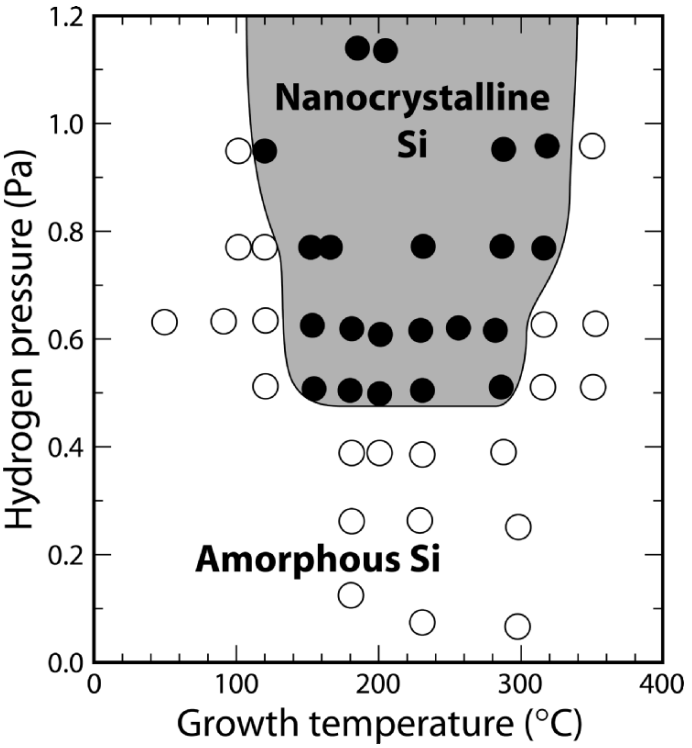

Figure 8.10: Experimental results showing how H_2 partial pressure and substrate temperature affect crystallinity in sputter deposition of a-Si:H in Ar-H_2 gas mixtures. Filled circles represent nanocrystalline Si while open circles correspond to amorphous Si. Figure courtesy J. Abelson, for discussion see Reference 11.

and by cosputtering Si and Ge targets simultaneously. The experimental results are shown in Figure 8.10. The process is the most easily controlled but not the only method for producing crystalline/amorphous transitions within a structure layer. When one introduces nanocrystalline regions in a device, the result is a doping profile with large variations in electrically active dopant concentration between the amorphous and nanocrystalline regions.

8.5 OPTICAL PROPERTIES

Optical absorption in tetrahedral crystalline semiconductors such as Si and GaAs shows variations with energy corresponding to variations in the bonds and the details of the density of states obtained from the energy-momentum relationships [see Section 2.1]. The lowest energy absorption derives primarily from transitions from

p to s orbitals on adjacent atoms in common semiconductors [Chapter 5]. When the same material is produced as a glass with tetrahedral subunits, the first and second nearest neighbor bonds are largely unchanged. This means that the basic absorption behavior is primarily unchanged, although distortions in bond angles modify the energies of absorption edges and maxima somewhat. Loss of organization at longer ranges blurs peaks in the absorption spectrum. As bond distortions cause states to move from the band edges into the gap, the effective gap for optical absorption generally increases. Finally, because amorphous materials cannot have indirect gaps, a transition from indirect to direct upon amorphization also involves a loss of dispersion with momentum direction and a change in density of states. For an indirect gap material such as crystalline Si, a conversion to amorphous would be accompanied by a loss of the low energy minimum, which can also lead to an expansion of the energy gap.

Absorption coefficient data and various contributing mechanisms of a typical amorphous semiconductor are shown in Figure 8.11. [12] There are three primary regions. The high absorption region I corresponds to absorption due to electron transitions across the mobility gap from delocalized (band like) states to other delocalized states. Typically, for band-like transitions as the photon energy approaches the mobility gap energy, the absorption coefficient exhibits a power-law decrease. Region II is absorption from band like states to band tail states or band tail to band tail transitions where the density of states is still rather high. In this region the absorption coefficient is typically falling exponentially. Region III is due to transitions to, from, or among localized states in the mobility gap and absorption is roughly constant.

For a free-electron system the band density of states decreases parabolically, as discussed in Chapter 2. The same parabolic decrease is also generally found in amorphous semiconductors. We know that a power-law expansion of any function around an extremum has quadratic dependence when sufficiently near the maximum or minimum point. Thus, it should not be surprising that the density of states follows a similar behavior in crystalline and amorphous materials. This quadratic behavior is exhibited in region I of Figure 8.11. An absorption edge can be defined based on fitting this portion of the absorption spectrum based on the function

$$\alpha(\nu) = b\left(h\nu - E_0\right)^2 \qquad 8.7$$

where E_0 is the absorption edge energy, hν is the photon energy, and b is a constant. Equation 8.7 assumes free-electron band edges. The true bands in amorphous semiconductors are not exactly parabolic and may distort this behavior to the point that a quadratic relationship is no longer observable.

In all semiconductors and particularly in amorphous materials there are states in the energy gap that decrease in density roughly exponentially as one moves into the gap. These are the band tails described earlier. The resulting absorption coefficient

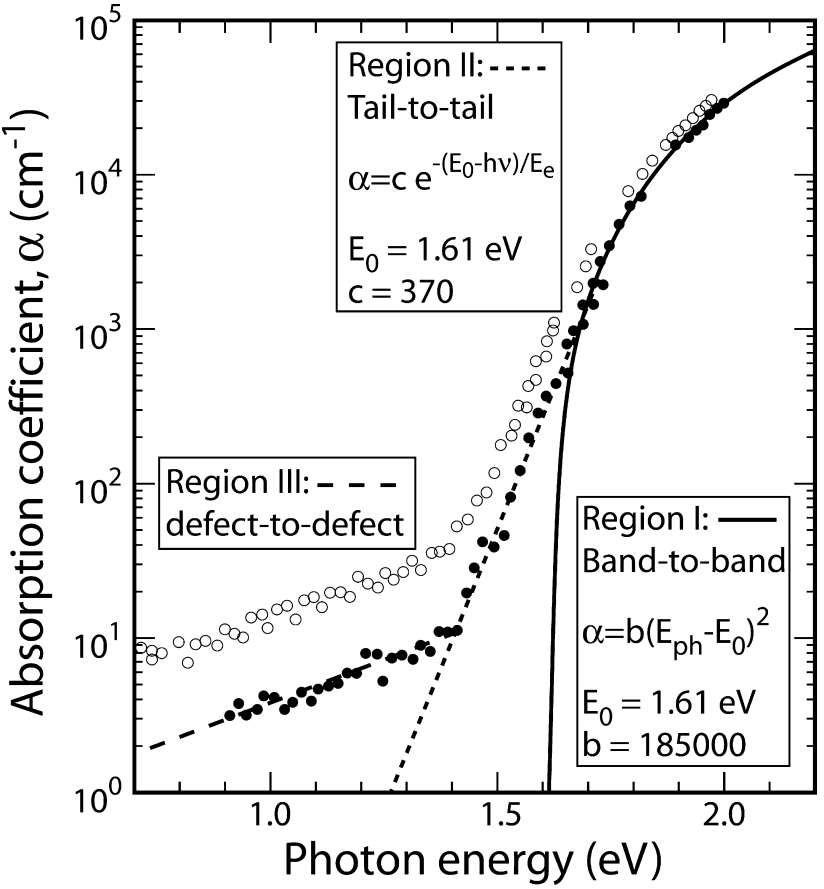

Figure 8.11: Optical absorption data for two a-Si:H films deposited by rf-PECVD using SiH_4 source gas. [12] Solid circles indicate as-deposited film results while open circles show the effect of annealing at 500°C for 30 min. Data was fit using Equations 8.7 (solid curve) and 8.8 (small dashed curve) for regions I and II. Region III also shows a simple exponential fit (larger dashes). The indicates shows that annealing increases the defect density in the film.

decreasing exponentially below the energy E_0 of Equation 8.7 can be written approximately as

$$\alpha(h\nu) = \text{const.}\, e^{-(E_{0'}-h\nu)/E_e} \qquad 8.8$$

where hν is the photon energy, $E_{0'}$ is the same as the parabolic energy edge and E_e is the characteristic width of the dominant band edge, typically <0.1 eV. The wider

band edge will set the apparent band-tail width and determine the absorption coefficient behavior. Which edge this is depends upon the details of the semiconductor involved. In a homopolar semiconductor such as amorphous silicon, the band tails will be relatively symmetrical with differences primarily resulting from the effective masses of the bands. In more complex ternary or multinary compound semiconductors, the sublattice on which the most substantial disorder occurs may determine the greatest band edge width. Various models have been proposed to explain the source of Equation 8.8 and can be found in Connell. [13] It is sufficient here to assume that the behavior is due to distorted localized bonds in the structure.

The optical gap (related to the mobility gap) in amorphous Si and other amorphous semiconductors exhibits temperature-dependent behaviors that are qualitatively similar to the temperature-dependences of crystalline materials. For example, a-Si:H shows a decrease in optical gap as temperature increases, as one would expect. Unlike the case for crystalline materials, the temperature dependence of a-Si:H is primarily related to changes in phonon-electron interactions. Thus, rather than a linear-quadratic relationship to temperature, one finds a change in optical gap of

$$E_{gap}(T) = E_{gap}(0) - \frac{2a_B}{e^{\Theta/T} - 1} \qquad 8.9$$

where a_B is the electron-phonon interaction strength and Θ is the effective temperature of phonons in the solid.

The effect of pressure on the optical gap in amorphous semiconductors also differs from the behavior of crystalline materials. In indirect-gap semiconductors we found a negative change in gap with increasing pressure in Si and some other materials due to increasing angular dependence of bonds at short distances. Direct gaps were all found to increase with increasing pressure due to greater orbital overlaps at shorter bond lengths. In amorphous semiconductors one finds an increasing gap with increasing pressure as expected for direct-gap materials. However, there can also be structural changes induced by increasing pressure that can lower the gap. The latter is observed in a-Si:H, while normal, positive changes in gap occur in a-Ge:H.

8.6 AMORPHOUS SEMICONDUCTOR ALLOYS

Amorphous semiconductors can be alloyed in exactly the same way as can crystalline materials, although not with as good results. Currently, the most common inorganic amorphous semiconductor alloys are a-(Si,Ge,C):H. These have been investigated in some detail and some are in use in select applications. The carbon alloys have proven less effective due to difficulty in reducing defect densities in the mobility gap, as discussed below. The mobility gap can also be adjusted by controlling the hydrogen content, as described above and shown in Figure 8.6, which has proven more effective for increasing the gap than the use of C to the maximum gap obtainable with hydrogen addition.

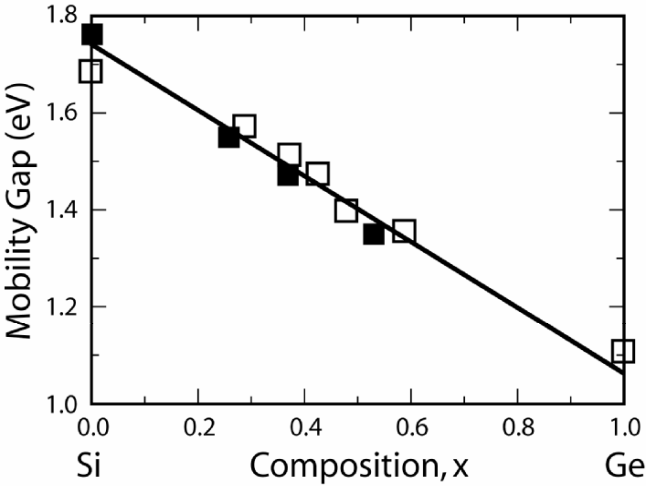

Figure 8.12: Shows typical values for mobility gap in a-$Si_{1-x}Ge_x$ alloys as a function of alloy composition at ~300K. Open points after Unold et al. [15]. Closed points after MacKenzie and Paul.[16] Numerous other sources of similar data also exist. Values vary somewhat with deposition conditions as might be expected from Figure 8.6.

From a consideration of the structure and bonding of amorphous materials, one can imagine how difficulties can arise. Consider the local bonding variations in crystalline alloys that normally cause bandgap bowing (see Chapter 6). Such variations will also occur in amorphous alloys and will change the energy of states in the material. Distortions in the amorphous network structure augment these effects. The alloy will therefore spread out the energies of distorted bonds more than in a non-alloyed material. Both broadening of the band edges and normal band-gap bowing can be expected in amorphous alloys. These two effects act in opposite ways, with an enhancement of states in the gap causing an increase in its width, while bowing reduces the gap. The counteraction of effects leads to less bowing in the amorphous alloys than in crystalline mixtures. The opposing effects also lead to broader Urbach edges and more states in the mobility gap. Such states can be the downfall of amorphous alloys in defect-sensitive devices.

As one would expect, Ge can be used to lower the mobility gap from 1.5-1.9 eV for a-Si to 0.9-1.0 eV for a-Ge in a continuous and relatively linear fashion. Figure 8.12 shows typical results for optical gap as a function of alloy composition. [15,16] Because, as discussed above, the mobility gap depends upon the structural distortions of the amorphous material as well as its composition, the mobility gap is also dependent upon the processing of the materials. Deposition processes using disilane

(Si_2H_6) as a Si source gas in a high H_2 partial pressure with careful control of ion bombardment of the growing film have been shown to produce relatively high-quality materials.

Amorphous Si/a-$Si_{1-x}Ge_x$:H alloy heterojunctions have band edge offsets as do crystalline materials. Roughly 80% of the change in energy gap is accommodated in the conduction band for this alloy.[17]

Unfortunately, deposition of a-$Si_{1-x}Ge_x$:H alloys with good properties is not straightforward. In poorly optimized processes, the addition of even modest amounts of Ge produces a large density of defect states in the mobility gap. The density of defects is generally found to increase exponentially with Ge content with an overall increase by a factor of ~3000 for a-Ge:H relative to a-Si:H for otherwise equivalent deposition conditions. This is true in all alloys studied to date, although some materials have lower defect densities overall across the range. One may understand why a-$Si_{1-x}Ge_x$:H shows a greater tendency to defect states when one considers the heats of formation for Si and Ge – 3.8 and 3.4 eV per molecule (78.44 and 88.04 kcal g^{-1} mol^{-1}), respectively. Thus, Si has ~10% stronger bonds that are, consequently, less inclined to strain or break. The resulting higher broken and distorted bond density in a-Ge:H explains the greater sensitivity to deposition conditions and the greater defect density. Indeed, in a-(Si,Ge) alloys, the majority of dangling bonds are from Ge atoms (90-99%). A delicate touch is required on the deposition process controls to obtain an equivalent defect density across the alloy range. Recipes for the production of a-$Si_{1-x}Ge_x$:H without significant increases in mobility edge width (a measure of material quality) have been obtained (although gap state densities still increase). Currently, alloys with Urbach energies of 45-50 meV, consistent with the values for unalloyed a-Si:H can be produced routinely with care and are sufficient for applications such as photovoltaic solar cells. Thus, a-$Si_{1-x}Ge_x$ has become an important alloy for band-gap engineered devices. Still, it is a difficult material to work with.

A-$Si_{1-x}C_x$:H alloys have also been explored as a possible means to increase the mobility gap. Indeed, very large increases in mobility gap have been achieved, at the price of massive defect densities. For example, an increase in mobility gap from 1.75 to 3 eV was obtained. [17] However, the increase in gap was highly dependent upon the hydrogen content of the alloy. It is not surprising that a-$Si_{1-x}C_x$:H alloys behave very differently from a-$Si_{1-x}Ge_x$. The crystalline Si-Ge alloy is completely miscible over the entire composition range so the bond energies and bonding configurations cannot be very different, nor is there a strong tendency to order the mixture to form a compound. Si and C, however, react to produce SiC, with little solubility of excess Si or C in the elemental Si or C or in the SiC compound. Consequently, it should not be unexpected that a-(Si,C) alloys show a large preponderance of Si-C bonds in preference to Si-Si or C-C bonds. A detectable minority of C-C bonds also occurs for C contents below 50%. This tendency to form a-SiC + a-Si two phase mixtures rather than forming a random alloy leads to a change in the energy band structure of the material, with large numbers of defect states due to localized disordering or variations

in the material chemistry. To picture this, consider an a-SiC matrix with a large energy gap but including localized Si-Si bonds with low energies. Such defects would appear in the mobility gap of the final structure. Being first-nearest neighbor bonds, they would be present regardless of their state of local distortion and would be unaffected by local hydrogen content. The situation is not quite this bad, as one needs a cluster of at least five Si atoms to make a reasonably a-Si-like region. However, the tendency of this alloy to phase separate leads intrinsically to trouble and poorly performing alloy materials.

8.7 APPLICATIONS

8.7.1 Thin film transistors

Amorphous semiconductors are employed where crystalline substrates are unusable or impractical such as when a large number of discrete devices need to be integrated onto the surface of a material such as glass. Even when a single-crystal substrate could be used the maximum area is limited to the size of a single-crystal substrate, while amorphous semiconductors are easily adapted to large substrates. Devices on flexible surfaces and on materials that cannot be heated significantly (polymers for example) are also commonly constructed from amorphous semiconductors.

Amorphous semiconductors are used in switching devices (mostly field-effect transistors), which must be made reliably on polycrystalline or amorphous surfaces, and solar cells (essentially simple diodes), which must be made in extremely large areas at the lowest possible cost on the least expensive substrate (glass for example) to have an acceptable price. These devices function well because for light-absorption and diode operation the mobility gap of an amorphous material acts essentially as does a normal semiconductor energy gap. Luminescent devices are not made from a-Si:H or other inorganic amorphous semiconductors because these do not emit photons at a well-defined energy, nor at all efficiently. Amorphous organic materials are used as light emitters, as discussed in the next chapter.

The most common application of amorphous semiconductors is in thin film transistors that drive “active matrix” liquid-crystal displays or large-area optical sensors. In display devices, electrodes control the orientation and/or twist of polar organic molecules in the liquid crystal. These, in turn, determine the polarization of light passing through the display. To improve the speed of the display and to reduce crosstalk between pixels or areas, transistor switches need to be integrated into each pixel. Because each pixel requires a separate transistor for control, and because the pixels are distributed across the entire display, the transistors must likewise be distributed. To fabricate all of these devices from crystalline bits, and position and contact each separately would be prohibitively complex and expensive. It is far easier to make transistors from amorphous Si on the glass surface of the display directly. This is how all current active-matrix liquid crystal displays are fabricated. In a video display, speed requirements are modest (switching times of a few

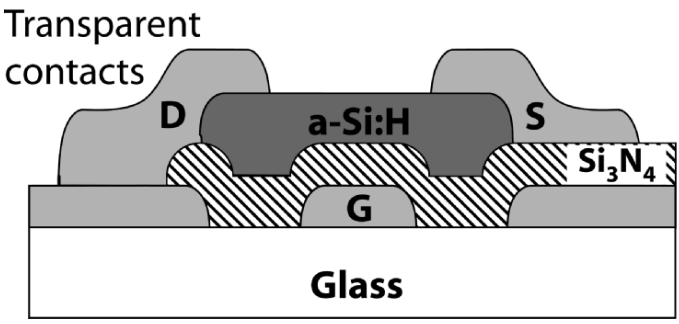

Figure 8.13: A schematic diagram of a typical thin film field-effect transistor using a-Si:H as the semiconductor. The configuration shown is known as the inverted staggered geometry, which is the most popular and highest performing structure. "Inverted" refers to the way the gate electrode and dielectric underlie the a-Si:H channel. "Staggered" indicates that the gate is on the opposite side of the semiconductor from the source and drain contacts. S, G, and D designate the source, gate, and drain contacts.

microseconds are sufficient). However, for most applications, power-efficiency is also important. Liquid crystal devices require very small amounts of power to operate. To prevent unintended turn-on and to minimize off-state power consumption, the maximum ratio of on-state to off-state current and the minimum off-state current are required. Amorphous Si TFT's meet these requirements well.

A second application for a-Si TFT's of growing importance is imaging systems acting as direct replacements for photographic film, especially in large-area medical systems such as x-ray instruments. These switch charge generated by local photosensors to amplifiers. This application also requires large ratios of on-state to off-state resistance and very high off-state resistances. As with liquid crystal displays, the speed of the device need only be fast enough to handle the sampling frequency of each pixel, typically a few milliseconds, or tens of kilohertz frequencies. Devices with low carrier mobilities and large trap state densities such as a-Si:H can still handle these switching rates adequately.

The typical a-Si:H thin film transistor (TFT) is a field-effect device, shown schematically in Figure 8.13. The electrodes are patterned on a glass substrate and the gate is covered by a dielectric, usually Si_3N_4. The active a-Si:H layer is added on top of the dielectric and the device is finished with source and drain electrodes. Application of a bias voltage to the gate controls channel conductivity as usual in field-effect transistors. These switch power onto and off of electrodes in displays quickly and efficiently.

More recent applications are beginning to require higher speeds, which a-Si:H devices with carrier mobilities of $< 1 cm^2\ V^{-1}s^{-1}$ are not always capable of meeting. This is driving movement away from amorphous semiconductors to nanocrystalline

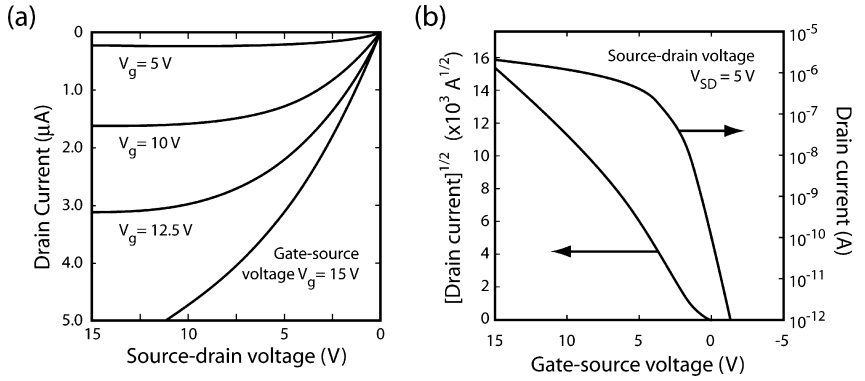

Figure 8.14: Characteristics for two a-Si:H thin film transistors. (a) The source-drain current as a function of source-drain voltage at several gate voltages for a transistor described in Powell [1989, Ref. 18] and (b) the source drain current as a function of source-gate voltage for a device described in Street [1998, Ref. 19]. Plotting data from [Powell, Ref. 18] on figure (b) shows a linear rather than quadratic behavior but a generally similar curve on the logarithmic scale. Note: compare these graphs with Figure 9.12 for an organic TFT.

materials with higher mobilities. The usual trade-off of converting to a nanocrystalline film is that higher mobilities are accompanied by higher leakage (off-state) currents. Therefore, there is still an important market for a-Si:H switching devices.

Typical results for a-Si:H TFT device characteristics are given in Figure 8.14. The critical parameter for current capacity is the width of the active region (in and out of the plane of Figure 8.13) relative to the length from source to drain. Higher widths at a given length increase current capacity at a given drive voltage and decrease on-state resistance. Typical width-to-length ratios are of the order of five. One of the features of the performance data evident in Figure 8.14 is the very high off-state resistance and high on-to-off state resistance ratio. a-Si:H TFT's can be produced with off-state resistances typically exceeding 10^{14} Ω and on-to-off current ratios exceeding 10^8. These properties are of great importance to the success of a-Si:H devices in display and imaging systems. The shape of the subthreshold current (the low current, low bias side of Figure 8.14b) can be modeled to provide an understanding of the density of states in the energy gap and the nature of the band tails in the material from which the TFT is produced.

a-Si:H TFT's are not without problems. Due to generation of carriers from trap states, current persists, decaying roughly inversely with time, after the device is nominally switched off. Therefore, the resistance appears to increase or the reverse

leakage current appears to decrease as time goes on. This makes the device switch slowly. Slow switching is not a major problem for most applications where speed is not critical. More significantly, the threshold voltage for turn-on of the device can vary over both long and short time scales, from device to device, and, most unfortunately, can have a history/memory effect. In the latter, injection of carriers results in increases in dangling bond density (the Staebler Wronski effect). These midgap states trap charge and can affect device capacitance, switching rate, and threshold voltage. This is a serious problem for device designers. In addition to charge-injection-induced increases in trap density, normally present and unchanging traps have history and time-dependent charges. In other words, trapped charge can take a significant amount of time to escape a trap. This leads to additional variations in threshold voltage. Finally, defects in the Si_3N_4 dielectric can trap additional charge and modify the threshold voltage. All of these defect behaviors lead to considerable variability in resulting devices, which can have a substantial impact on the yield and performance of large-area devices.

The lesson of the thin film transistor is that amorphous semiconductors work well when the demands on the performance of the device are not great and where light emission is not important. When such requirements are coupled with restrictions on the surface on which the material is to be applied, amorphous semiconductors can become essential. The major question at this point is becoming – will organic materials replace inorganic materials in amorphous thin film devices?

8.7.2 Solar cells

Solar cells are diodes which, when exposed to light, produce an electric current. The concept is very similar to operation of a light-emitting diode in reverse, and was discussed in Chapter 6 for crystalline materials. Here we turn to non-crystalline solar cells. A-Si:H is the most widely manufactured material for thin film solar cells, although other materials are rapidly approaching it in production volume, because it can be deposited by relatively straightforward techniques onto glass or other materials coated with a transparent conductor. This is much less costly than single-crystal devices such as GaAs-based solar cells. As noted above, it is difficult to dope a-Si:H p or n type. Therefore, most a-Si:H solar cells are p-i-n structures. In other words, they consist of a thin, highly p-type region, a thick undoped region, and another thin n-type region. This is good because the p and n regions can be optimized for high doping, while the i-layer can be adjusted for best carrier collection. Generally, the deposition conditions under which these two behaviors are obtained are very different.

A typical a-Si:H single-junction solar cell along with its operating characteristics are shown schematically in Figure 8.15. In a crystalline solar cell the optimal energy gap for maximum efficiency is between 1.4 and 1.5 eV. In a-Si:H devices the optimal value may be somewhat higher, closer to 1.8 eV, if the device does not collect current well. Fortunately, it is easy to produce a-Si:H with a mobility gap energy near the optimal value.

A significant advantage of a-Si:H and alloys with Ge and C is that these are direct-gap materials, unlike their parent crystalline semiconductors. Consequently, they have at least 100 times higher optical absorption coefficients than the equivalent crystalline materials. The benefit is that only 1% of the thickness of the crystalline devices is required to absorb an equivalent amount of light. At the same time, one needs carriers to move only 1% as far as in crystalline Si or Ge before they reach a contact. Therefore, the electrical quality of the material may be much lower and carriers can still be collected. For a-Si:H the very high absorption coefficient allows all light to be collected in ~1μm of material. This means it needs only a relatively thin film of a-Si:H to produce a useful device. Hence the name thin film solar cells.

In the simulated device shown in the Figure 8.15 the current/voltage curve under light exposure has a lower resistance in forward bias than the curve without light (the light and dark curves cross). This crossover is the signature of a photoconductive response in the device – under light the amorphous semiconductor becomes more conductive. The slope of the curve at zero voltage can indicate a shunt in the junction allowing current to pass in spite of the resistive response of the diode. In the simulated device, however, this simply indicates a voltage-dependent collection of current. If there were a real shunt in the device then the dark current curve would also show the same or nearly the same resistance and hence current as a function of voltage.

If the absorber material is of high quality, primarily meaning that it has relatively few defect states in the gap, then the built-in electric field will transition continuously and uniformly from one contact to the other through the i-region. This maximizes the

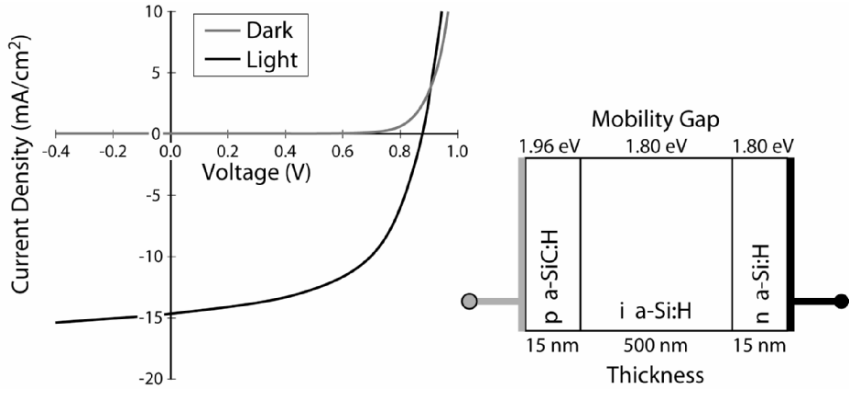

Figure 8.15: Simulated current/voltage curves calculated using the AMPS computer code [20] based on a standard simulation supplied with the code. Notice that the light curve crosses the dark one indicating that the device exhibits photoconductivity.

field assisting collection of carriers where they are generated and produces the best solar cell. If the defect density is high, as in poor material, the field is localized near the contacts. Field localization has several effects. The two most significant are that the electic field in the bulk of the i-layer is reduced, leading to less current generation by the device, and that in forward bias without photogeneration (in the dark) current injection at the contacts becomes space charge limited.

This latter point deserves emphasis. As we will see in organic devices, any time that carriers are injected from a contact into a very-low-mobility material they will tend to pile up near the contact (creating a "Coulomb blockade"). As their mobility is low, they may be unable to diffuse away into the bulk of the low-mobility layer as fast as they are injected. The resulting pile-up creates a field near the contact that tends to reject additional injection, effectively increasing the contact resistance at high current levels. This condition is known as space-charge-limited injection, and also occurs at heated cathode surfaces under some conditions. Two devices with and without space charge limited injection are compared schematically in Figure 8.16.

If the solar cell is produced from good material, mobilities are relatively high as are carrier diffusivities. Therefore, space-charge limitations are insignificant and the device works well. If the carrier mobility is low then carrier collection is poor

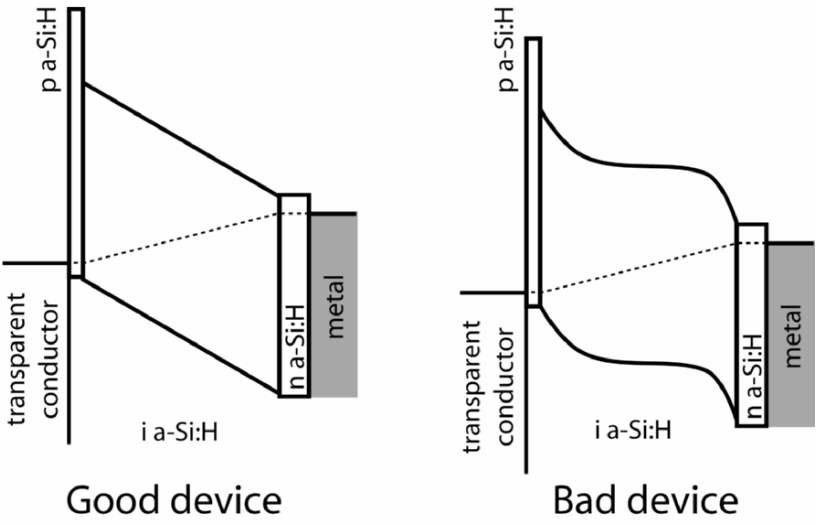

Figure 8.16: Band edge diagrams for good and bad a-Si:H solar cells similar to the one in Figure 8.15 showing the effect of increased defect density in the i-region. The p-type region is shown with a higher gap to prevent electrons from escaping to the transparent contact.

and the device yields both low currents and low voltages. One may reduce contact injection problems by using a nanocrystalline rather than an amorphous semiconductor at the contact. The nanocrystalline material has a higher mobility and is easier to dope heavily.

One of the greatest limitations to the application of a-Si:H in solar cells is the Staebler-Wronski effect, mentioned above. This is a light- or current-injection-induced enhancement in defect state density in the material. Because performance of the solar cell is reduced by increasing the defect density, the solar cell degrades during operation. Atomic-scale mechanisms for this degradation continue to be hotly debated but are most likely the result of a rearrangement of hydrogen atoms or a reorganization of dangling bond states such that the dangling bonds become more electrically active. Although the device performance recovers to nearly its initial value with proper treatment (usually annealing at moderate temperatures will suffice), the degradation reduces the photovoltaic conversion efficiency by up to two percent (for example, from ten to eight percent efficient). Even more annoying is that better devices are more susceptible to this phenomenon because the poor devices have so many defects to begin with. Products can only be specified to operate at the degraded level, even though they may initially produce higher powers.

The current technology for amorphous solar cells involves three diode junctions in series, each collecting the energy from a successively longer wavelength portion of the solar spectrum as one passes from the top to the bottom of the device. Each junction has a progressively lower mobility gap and is transparent to light below the mobility gap energy. Whatever light passes through one device is available to the next, if its energy exceeds the mobility gap energy of that material. The current produced by each junction is set by the number of photons in the portion of the solar spectrum that it absorbs and its collection efficiency. This current is designed to be the same for each device since they are wired in series. The voltage that each device produces is some fraction of its mobility gap. The voltages add when the devices are wired in series. The output power is then the product of current and voltage at a given load. The concept of a multijunction solar cell and how it divides the solar spectrum are shown schematically in Figure 8.17.

To accomplish voltage addition in a multijunction device, one must arrange an n-p "tunnel" junction between each device, as shown in Figure 8.17. The purpose of this junction is not to produce a working diode. Rather the diode should break down due to tunneling to provide an ohmic contact from device to device and convert smoothly from one type of majority carrier to the other, forcing all minority carriers to recombine. At the same time, it is transparent, which would not be the case with a metal-to-metal contact. It has been primarily the progression from single to double to triple junction devices that has been responsible for the gains in efficiency of a-Si:H solar cells in recent years.

Selection of the three energy gaps varies and the optimal values depend upon the performance of each junction and the light conditions for which performance is to be optimized. The overall objective of this design is to ensure that each device produces as nearly the same current as possible at the maximum power output voltage. Values shown in Figure 8.17 are schematic and not representative of a particular device. Multijunction devices are also commonly used in single crystalline solar cells based on III-V type semiconductors and are being explored for use in polycrystalline thin film devices. It should be noted that each device in the structure must be a good solar cell (at least in terms of current generation) if the multijunction solar cell is to be more efficient than a single-junction device of the same quality. If one device is

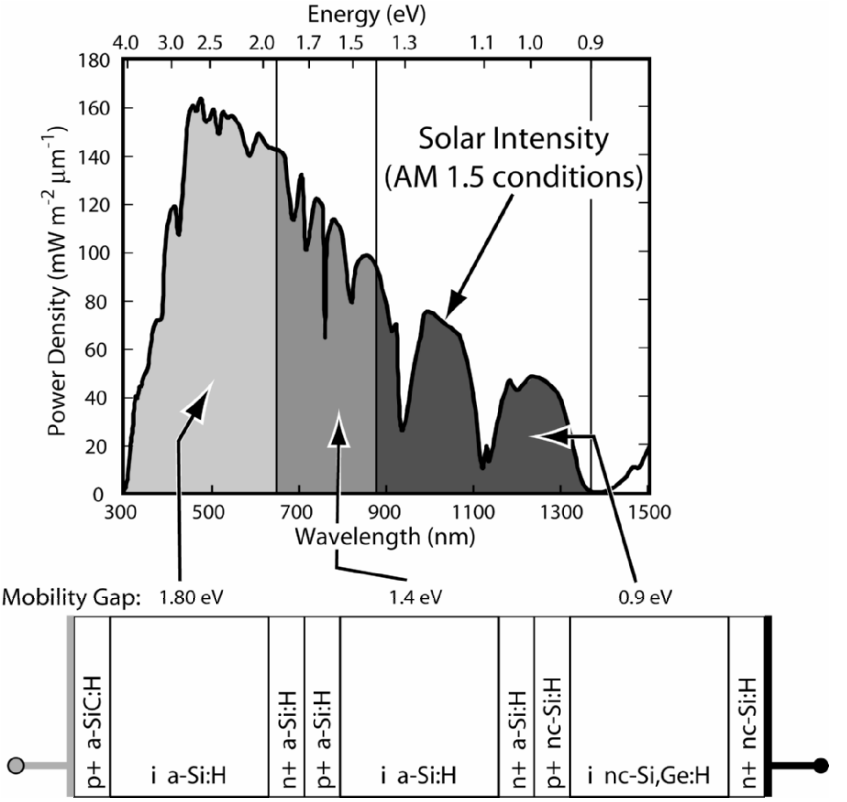

Figure 8.17: A schematic diagram showing how a triple junction solar cell might collect current from photons in different parts of the solar spectrum. Light enters the device from the left through the wide-gap solar cell and portions of the spectrum penetrate into the underlying devices.

poor, producing little current, then for the other solar cells to drive their output current through it they have to forward bias the bad device. This leads to net power dissipation in the bad junction rather than net power production.

The requirement for progressively lower energy gaps is met in common structures by two layers deposited with different H contents, and consequently having different gaps, adjusted as in Figure 8.6, and a third layer consisting of a Si, Ge alloy. Other devices are constructed using a-Si:H only for the wide-gap layer with Si, Ge alloys for both narrower gap regions. Still another approach is to produce nanocrystalline layers for a narrow-gap junction in the device. The latter is one of the most popular approaches currently.

Nanocrystalline materials for absorber layers (as opposed to just contact regions) have the advantage of higher carrier mobility than amorphous materials. Devices utilizing them for the narrow-gap structures tend to produce higher currents (fewer defect states are present to mediate recombination) and have less tendency to light or forward-bias-induced degradation. At the same time, the lower absorption coefficient, resulting from the indirect gap, requires both thicker layers and a reflective back contact to scatter and return as much of the light that fails to be absorbed as possible back into the nanocrystalline layer. A good back contact reflecting and scattering light into the nanocrystalline absorber can dramatically enhance the response of the device, especially at long wavelengths where absorption is lowest.

In single-junction microcrystalline Si:H solar cells the open circuit voltage and sharpness of the diode turn-on curve (the “fill factor”, being the ratio of the maximum power obtainable from the device to the power represented by the product of open circuit voltage and short circuit current), both decrease with device thickness. Voltage decreases because the number of defects increases between where carriers are generated and the contacts where they are collected. Fill factor decreases because of series resistance in the junction. At the same time the short-circuit current increases as the material available for photogeneration increases.

Because each device in a multijunction structure absorbs only a part of the solar spectrum, each produces less current than an optimized single junction device would. It is important to remember that lower-current devices are generally more sensitive to defects, because recombination and trap states are less likely to become saturated with carriers. This means that multijunction devices tend to be more sensitive to material quality. In amorphous devices it also means that light-induced degradation is more of a problem. This is another reason to use nanocrystalline materials for the narrow-gap device.

8.8 SUMMARY POINTS

- Coordination of atoms in inorganic amorphous semiconductors is usually either two-fold (chain-like structure) or four-fold (tetrahedron based structure).
- Tetrahedron-based structures consist of randomly-organized networks of tetrahedrally-coordinated atoms. Bonding distortions are primarily in bond angle rather than bond length.
- Amorphous semiconductors must have direct mobility gaps.
- Highly distorted and dangling bonds result in a continuum of states in the energy gap. These come primarily from the band edge density of states of the equivalent crystalline structure.
- Defect-related states in the energy gap are increasingly widely separated in space as the distortion increases and they move farther into the gap. At some point the separation leads to a sudden decrease in carrier mobility among the defect states.
- Therefore, there is a "mobility gap" equivalent to an energy gap in a crystalline material which functions, for device modeling purposes, exactly as does a true energy gap in a crystalline device.
- Band tails resulting from an exponentially decreasing density of states are observed around the mobility edges. Wider tails with higher density of states result in lower-performance devices.
- Discrete states distributed across the gap occur. Higher densities of these states lead to lower carrier mobilities and higher minority carrier recombination and trapping rates.
- Dangling bonds tend to result in states near the middle of the gap. Hydrogen atoms may effectively passivate these bonds moving the states out of the mobility gap.
- Hydrogen concentration may be used to control the magnitude of the mobility gap in a-Si:H. Increasing hydrogen increases the mobility gap energy.
- Defect states in the gap make doping difficult.
- Doping may be improved by using nanocrystalline material for the heavily doped regions.
- Optical absorption has three distinct regions associated with: states outside the mobility gap, band-tails, and discrete states.
- Mobility gaps vary with temperature differently from crystalline material energy gaps.
- Generally one observes "dispersive transport" in which the mobility for each carrier is different with some carriers moving very well but with the average carrier moving very poorly.
- Deposition of a-Si:H and related materials is most commonly performed by chemical vapor deposition enhanced with a plasma or hot wire. Sputtering is also used.

- Doping is accomplished by adding B, As, or P to a-Si:H and related materials. Doping efficiency is generally low requiring very high concentrations of dopant to move the Fermi level in the mobility gap. Better materials are more easily doped.
- Nanocrystalline materials may be produced controllably by modification of deposition conditions. These have narrower and in the case of Si-Ge alloys indirect energy gaps.
- Carrier mobilities are higher and absorption coefficients lower in nanocrystalline indirect-gap materials.
- a-$Si_{1-x}Ge_x$:H alloys can be produced by codeposition of the elements. These have lower mobility gaps than a-Si:H and much higher defect state densities (increasing exponentially with x).
- a-(Si,Ge,C):H can be produced with C increasing the gap.
- Generally adjusting H content is more effective for gap increase than adding C because of additional defect states added with alloying with C.
- Little band-gap bowing occurs in amorphous semiconductor alloys and most band offset in Si-Ge alloys occurs in the antibonding (conduction) band.
- Low mobility materials often suffer space-charge-limited carrier injection at contacts in which contact resistance increases at high current densities.
- The Staebler-Wronski effect is the result of an increase in states in the mobility gap and leads to lower carrier mobilities, higher trapping and recombination rates, and worse device performances. It is the result of minority carrier injection into the amorphous material either through forward bias carrier injection or through optical generation by light.
- Thin film transistors (TFTs) are used for display applications in which large numbers of transistors are needed, distributed across a non-single-crystalline substrate.
- TFTs are generally field-effect devices in which only the channel is an amorphous semiconductor.
- a-Si:H TFTs have high off-state resistances and high on-to-off state current ratios.
- Switching speed in a-Si:H devices is generally related to carrier mobility and trap state density leading to a preference for nanocrystalline materials.
- a-Si:H solar cells are interesting as they can be produced in large areas on inexpensive substrates by simple processes.
- Amorphous solar cells are usually p-i-n structures with high doping levels in the p and n regions and the i-region optimized for higher mobility and low gap state density.
- Multijunction solar cells divide the solar spectrum into segments of increasing energy. Each junction absorbs a lower portion of this spectrum. These devices have higher efficiencies if each junction performs well but are more sensitive to defect state density.

8.9 HOMEWORK

1) Explain briefly why a-Si:H has a much higher absorption coefficient near the mobility gap energy than crystalline Si has.

2) Explain quantitatively why optical absorption

   a) increases as the square of the photon energy above the mobility gap.
   b) decreases exponentially with energy below the mobility gap energy.

3) If the defect density is constant across the majority of the mobility gap below the band tail region why does the absorption coefficient decrease as the photon energy decreases? What would you expect the mathematical dependence to be?

4) If the most common minority carrier in an amorphous material does not move, how can current be transported?

5) Describe the three mechanisms of carrier transport in amorphous semiconductors.

6) What is the Staebler-Wronski effect and why is it important in amorphous solar cells?

7) What is the best way to adjust the mobility gap in an amorphous semiconductor and why is this superior to alloying?

8) Why is band gap bowing not observed significantly in a-$Si_{1-x}Ge_x$:H?

9) Why is the mobility gap in a-Si:H greater than the energy gap in crystalline Si?

10) How does hydrogen help improve the electrical properties of a-Si?

8.10 SUGGESTED READINGS AND REFERENCES

Suggested Readings:

Brodsky Marc H., *Amorphous Semiconductors* in *Topics in Applied Physics*, volume 36. Berlin: Springer-Verlag, 1979.

Cohen J. David "Light-induced defects in hydrogenated amorphous silicon germanium alloys." Solar Energy Mater. & Solar Cells 2003; 78: 399-424.

Conde J.P., Chu V., Shen D.S., Wagner, S. "Properties of amorphous silicon/amorphous silicon-germanium multilayers." J. Appl. Phys. 1994; 75: 1638-1655.

Willardson R.K., and Beer, Albert C., *Semiconductors and Semimetals*, v. 21: Hydrogenated Amorphous Silicon. New York: Academic Press, 1984.

N.F. Mott, "Electrons in Non-crystalline Materials", in *Electronic and Structural Properties of Amorphous Semiconductors*, P.G. Le Comber and J. Mort, editors. (Academic, New York, 1973), p.1.

Zallen, Richard, *The Physics of Amorphous Solids*. New York: Wiley, 1983.

References:

[1] Kramer B and Weaire D., "Theory of electronic states in amorphous semiconductors," in Brodsky M.H., *Amorphous Semiconductors* in *Topics in Applied Physics*, v. 36. Berlin: Springer-Verlag, 1979.

[2] Lecomber, P.G. and Spear, W.E., "Doped Amorphous Semiconductors," in Brodsky M.H., *Amorphous Semiconductors* in *Topics in Applied Physics*, v. 36. Berlin: Springer-Verlag, 1979.

[3] Dawson, R.M.; Li, Y.; Gunes, M.; Nag, S.; Collins, R.W.; Bennett, M.; and Wronski, C.R.; "Optical properties of the component materials in multijunction hydrogenated amorphous silicon based solar cells." Guimaraes, Leopoldo, editor, *Proc. 11th European PV Solar Energy Conference and Exhibition*, Montreux, Switzerland, October, 1992. Chur, Switzerland: Harwood Academic Publisers, 1993: 680-3.

[4] Staebler, D.L. and Wronski, C.R., "Reversible conductivity charge in discharge-produced amorphous Si." *Appl. Phys. Lett.*, 1977; 31: 292-4.

[5] Nagles P. "Electronic transport in amorphous semiconductors," in Brodsky M.H., *Amorphous Semiconductors* in *Topics in Applied Physics*, v. 36. Berlin: Springer-Verlag, 1979.

[6] Mott N.F. "Conduction in non-crystalline systems. IV. Anderson localization in a disordered lattice." *Phil. Mag.*, 1970; 22: 7-29.

[7] Mott N.F., "Conduction in non-crystalline materials. III. Localized states in a pseudogap and near extremities of conduction and valence bands." *Phil. Mag.*, 1969; 19:835-52.

[8] Zallen, Richard, *The Physics of Amorphous Solids*. New York: John Wiley & Sons., 1983.

[9] Paul W., Chen J.H., Liu E.Z., Wetsel A.E., Wickboldt P., "Structural and electronic properties of amorphous SiGe:H alloys." *J. Non-cryst Solids*, 1993; 164-6: 1-10.

[10] Unold T., Cohen J.D., and Fortman C.M. "Electronic mobility gap structure in deep defects in amorphous silicon-germanium alloys." *Appl. Phys. Lett.*, 1994; 64: 1714-6.

[11] Feng G., Kaytyar M., Yang Y.H., Abelson J.R., Maley N., "Growth and structure of microcrystalline silicon by reactive DC magnetron sputtering." Thompson, M.J.; Hamakawa, Y.; LeComber, P.G.; Madan, A.; Schiff, E.A., editors, *Amorphous Silicon Technology – 1992*, Proc. Mater. Res. Soc., v. 258, Pittsburgh, Pennsylvania: Materials Research Society, 1992: 179-84.

[12] Based on data from Cody, G.L. "The optical absorption edge of a-Si:H" in Willardson R.K., and Beer, Albert C., *Semiconductors and Semimetals*, v. 21: *Hydrogenated Amorphous Silicon, Part B: Optical Properties*, Jacques I Pankove, ed. New York: Academic Press, 1984.

[13] Connell, G.A.N. "Optical properties of amorphous semiconductors" in Brodsky M.H., *Amorphous Semiconductors* in *Topics in Applied Physics*, v. 36. Berlin: Springer-Verlag, 1979.

[14] Smith F.W., "Optical constants of a hydrogenated amorphous carbon film." *J. Appl. Phys*., 1984; 55: 764-71.

[15] Unold, D.; Cohen, J.D.; and Fortmann, C.M. "Electronic mobility gap structure and deep defects in amorphous silicon-germanium alloys", *Appl. Phys. Lett.*, 1994; 64: 1714-6.

[16] MacKenzie, D.W. and Paul, W., "Comparison of properties of a-$Si_{1-x}Ge_x$:H and a-$Si_{1-x}Ge_x$:H:F" in Madan, A.; Thompson, M.; Adler, D.; and Harnakawa, Y., editors, *Amorphous Silicon Semiconductors – Pure and Hydrogenated*. Materials Research Society Symposium Proceedings 1987; 95: 281-92.

[17] Conde, J.P.; Chu, V.; Shen, D.S.; Wagner, S., "Properties of amorphous silicon/ armorphous silicon-germanium multilayers." *J. Appl. Phys*., 1994; 75: 1638-55.

[18] Powell, M.J. "The physics of amorphous-silicon thin-film transistors." *IEEE Trans. on Electronic Devices* 1989; 36: 2753-63.

[19] Street, R.A. "Large area electronics, applications and requirements." *Phys. Statu Solidi a* 1998; 166: 695-705.

[20] McElheny, P.; Arch, J.; Lin, H.; and Fonash, S. "Range of validity of the surface-photovoltage diffusion length measurement: a computer simulation." *J. Appl. Phys*., 1988; 64: 1254:65; and Zhu, H. and Fonash, S.J. "Computer simulation for solar cell applications: understanding and design" and references therein. *Amorphous and Microcrystalline Silicon Technology-1998* Schropp, R. et al. editors, Proc. Mater. Res. Soc., v. 507, Pittsburgh, Pennsylvania: Materials Research Society, 1998: 395-402.